[4] Babcock, C. D. and Sechler, E. E., "The effect of initial imperfections on the buckling stress of cylindrical shells," NASA TN D-2005 (1963).

[5] Heise, O., "Die experimentelle Ermittlung der Beullasten von längsgedrückten dünnwandigen Kreiszylinderschalen," Deut. Ber. Forschungsanstalt Luftfahrt 214 (1963).

[6] Almroth, B. O., Holmes, A. M. C., and Brush, D. O., "An experimental study of the buckling of cylinders under axial compression," Lockheed Missiles and Space Co. Rept. LMSC 6-90-63-104 (1963).

[7] Tennyson, R. C., "A note on the classical buckling load of circular cylindrical shells under axial compression," AIAA J. 1, 475–476 (1963).

Normal Spectral Emissivity of Isotropic and Anisotropic Materials

G. W. Autio* and E. Scala†
Cornell University, Ithaca, N. Y.

THE effects of crystallographic orientation, at or near the surface, upon the emission of radiant energy have not been sufficiently studied. The current investigation is being made on a number of isotropic and anisotropic materials. The results for high-purity single crystal nickel and pyrolytic graphite are discussed herein. The high anisotropy of pyrolytic graphite allows one to readily examine the orientation effect upon $\epsilon_{n\lambda}$, the normal spectral emissivity. The "ity" ending is used because the specimen surfaces are highly polished and the materials are of excellent purity and soundness. The available literature indicates that very little investigation has been made of the normal spectral emissivity of single crystal nickel, pyrolytic graphite, and polycrystalline graphite in the near infrared region of the electromagnetic spectrum.

A schematic of the experimental apparatus employed is shown in Fig. 1. Four specimens can be embedded in the top of a high-purity and dense graphite block with good thermal contact. The blackbody cavity is a drilled hole in this graphite block of depth to diameter ratio of 6.75. Any one of the specimens or the blackbody cavity can be aligned with the water-cooled sight tube by rotating the control rod. Measurements are made sequentially by pulling up the graphite block to within about 0.050 in. from the end of the sight tube. That is, after each reading of a specimen or the blackbody, the graphite block is lowered to the uniform hot zone. The radiant energy is focused into the monochromator entrance slits by means of a spherical and a plane mirror. The same optical path is used for all specimens and the blackbody cavity.

With the specimen in the down position, at equilibrium temperature, the recorded millivolt level represents reflected and extraneous radiation as well as that emitted by the specimen. As the specimen is drawn up to the sight tube, a sharp decrease is recorded, until the radiant energy emitted by the specimen alone is obtained. The trace is linear between these points for about 3 sec, after which the slope deviates from linearity, representing the cooling of the specimen. The possible error due to radiant energy from the furnace tube walls is kept to a minimum by maintaining the smallest gap feasible without contact. Since the blackbody cavity reflects essentially no radiation, the change in its millivolt level is small (<0.10 mv) compared to a specimen (>1.0 mv) as the cavity is drawn up to the sight tube. The normal spectral emissivity of the specimen is the ratio of the millivolt reading of the specimen to that of the blackbody cavity for the same wavelength setting on the monochromator drum.

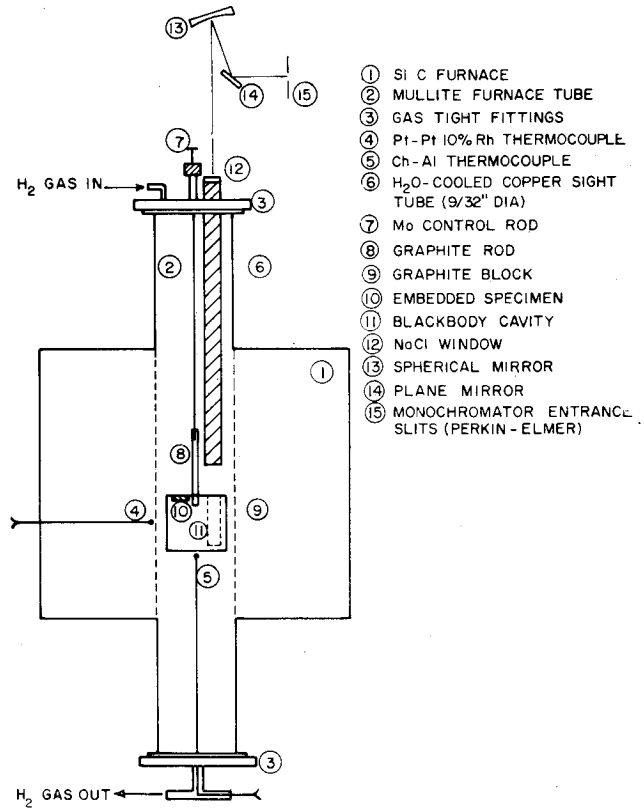

Fig. 1 Furnace schematic.

This technique has four desirable features: 1) the blackbody cavity and all specimens are as one unit under the same heating conditions; 2) the same optical path is used for the blackbody cavity and all specimens; 3) the measurements are strictly relative to the well-defined blackbody cavity; and 4) the optics employed are relatively simple. Whereas other techniques[1] may permit smaller errors of absolute measurement of emissivity, the method employed here allows for excellent comparative measurements on specimens of different crystallographic orientation. Normal spectral emissivity data for polycrystalline and single crystal nickel, pyrolytic graphite, and polycrystalline graphite are compared in Figs. 2–4. Data for these and other materials at temperatures down to 800°C have also been obtained.

The pyrolytic graphite is a Supertemp material formed at about 2150° C to a thickness of about 0.375 in. The polycrystalline nickel is the high-purity 270 grade (Huntington Alloy Products Division). The single crystal nickel (0.750-in. diam) was grown from the 270 grade by B. F. Addis in J. L. Gregg's Crystal Growing Laboratory at Cornell University. The measurements were performed in a hydrogen atmosphere to prevent any surface changes due to oxidation and the anomalous surface effects observed in vacuum or "neutral" gases. Photomicrographs (up to 1000×), interference photographs and x ray, back-reflection, and transmission Laue patterns were taken of all the specimens before and after the experiments to check the orientations and surface changes. In the results reported here, the specimens showed no evidence of orientation or surface changes.

The data on polycrystalline nickel compares favorably with the published results of Hurst,[2] Seban,[3] Ward,[4] Price,[5] and Reid[6] (Fig. 2). For polycrystalline nickel, there is agree-

Received August 13, 1964; revision received September 10, 1964. This technical note is part of a thesis to be submitted by G. W. Autio in partial fulfillment for the M. S. degree at Cornell. This research is supported by the Advanced Research Projects Agency.

* Research Assistant.
† Professor. Member AIAA.

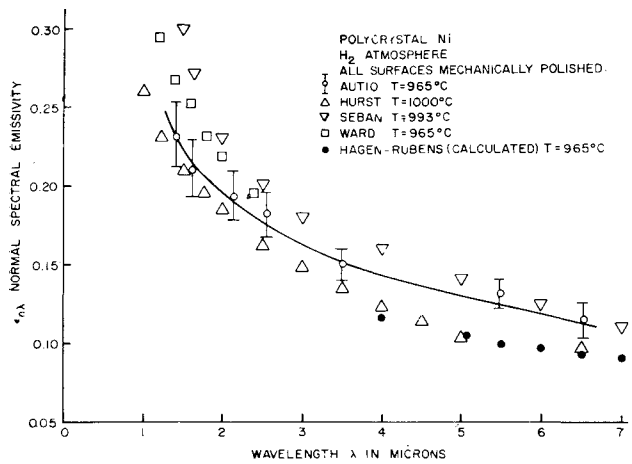

Fig. 2 Nickel reference data.

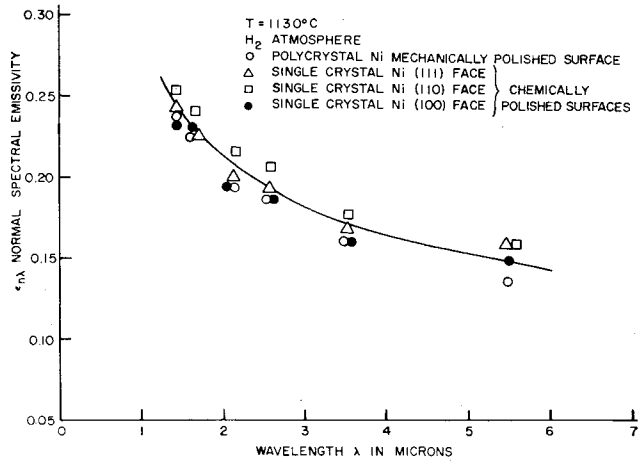

Fig. 3 Nickel orientation data.

ment in the experimental data with the Hagen-Rubens calculated curve beyond $\lambda = 5\ \mu$. The Hagen-Rubens[7] relation, which applies the Drude[8] theory in the infrared, has found fair agreement with experimental data. This equation relates the normal spectral emissivity with the d.c. electrical resistivity of a metal in the infrared

$$\epsilon_{n\lambda} = 36.50(\rho/\lambda)^{1/2} \qquad (1)$$

where $\epsilon_{n\lambda}$ is the normal spectral emissivity, ρ is the d.c. electrical resistivity in ohm-centimeters, and λ is the wavelength in microns.

The crystallographic orientation effect on $\epsilon_{n\lambda}$ was examined by comparing the emission of radiant energy from the polycrystalline nickel surface with three specimens of different orientations [(111), (110), and (100) faces]. The results in Fig. 3 indicate that, within the limits of error of the experiments, the emissivities are the same for all the nickel specimens from 1.50 to 6 μ at temperatures up to 1130°C. This is the expected behavior of a cubic metal which retains its isotropic properties at elevated temperatures. In order to demonstrate the significance of surface preparation, the emissivities were also compared for thermally etched, mechanically polished, and chemically polished polycrystalline and single crystal specimens, respectively, all with "optically smooth" surfaces. The results were identical, with no significant effects of grain boundaries. The emission of radiant energy, being essentially a bulk and not a surface characteristic, should not be changed as long as the surface is not chemically altered or made "nonoptically smooth."

In contrast, pyrolytic graphite represents a highly anisotropic material. Crystallographically, an *A* face designates the surface of a specimen wherein the majority of the graphite crystallites are oriented so that their "*c*" axes are parallel to the specimen surface. A *C* face means that a majority of the crystallites are oriented so that their basal planes or "*a*" axes are parallel to the surface. The *C* face also corresponds to the as-deposited surface for pyrolytic graphite material.

The results in Fig. 4 illustrate the effect of the high degree of anisotropy of the pyrolytic graphite. The radiant energy emitted from the *C* face is a factor of 2 to 3 lower than the *A* face. The carbon atoms are bonded by weak Van der Waals forces between the basal planes (along the "*c*" axis) compared to the stronger covalent bonding within the basal planes (along the "*a*" axis). The "*a*" axis has a lower d. c. electrical resistivity value with a consequent lower emission of radiant energy normal to this direction. It must be kept in mind that emission of radiant energy along the "*c*" axis, that is, normal to the *C* face, corresponds to the resistivity along the "*a*" axis parallel to the *C* face. The resistivity is taken in the direction of the electric vector which, in an electromagnetic wave, is perpendicular to the propagation vector. If the propagation vector is normal to a given face, then the corresponding resistivity value is taken parallel to the face. The electrical resistivity along the "*a*" axis is indeed orders of magnitude lower than along the "*c*" axis for pyrolytic graphite.[9] Thus, the Hagen-Rubens relation appears to hold qualitatively for pyrolytic graphite in that the higher emissivity face corresponds to the higher resistivity face. Further studies of graphites and other anisotropic materials are in progress.

An interesting trend in the results (Fig. 4) is that the *A* face pyrolytic graphite and polycrystalline graphite are almost "graybody" in behavior as compared to the *C* face pyrolytic graphite, which behaves more like a typical metal. By definition, "graybodies" exhibit normal spectral emissivities which are wavelength independent, whereas most metals have low normal spectral emissivities that decrease with increasing wavelength in accordance with a Hagen-Rubens relation in the infrared.

The large difference between the two pyrolytic graphite faces shows that the emission of radiant energy from a real body is not a surface phenomenon for "optically smooth" surfaces, but does indeed depend upon the crystallographic orientation of the material. The polycrystalline graphite surface is the strongest emitter of radiant energy of the three graphite specimens examined. However, this is most likely due to the many small pits that remained on its surface after a carefully polished surface was prepared. These small pits act as blackbody cavities that increase the amount of radiant energy emitted from the polycrystalline specimen.

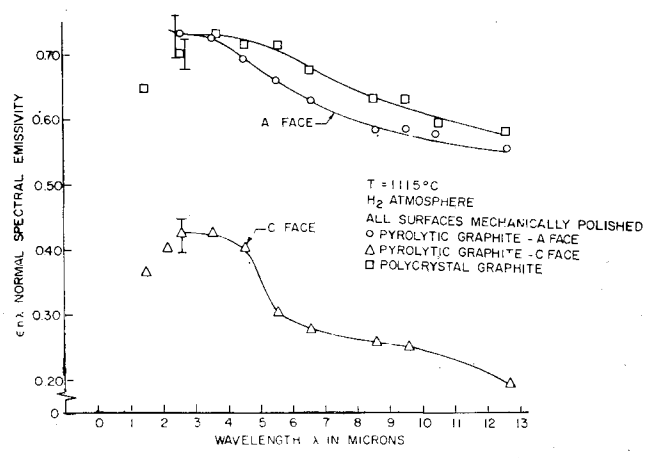

Fig. 4 Graphite data.

References

[1] Richmond, J. C., *Measurement of Thermal Radiation Properties of Solids*, NASA SP-31, Sessions IV and V, pp. 289–584 (1963).

[2] Hurst, C., "The emission constants of metals in the near infrared," Proc. Roy. Soc. (London) **142A**, 466–490 (1933).

[3] Seban, R. A., "System for the measurement of spectral emittance in an inert atmosphere," *Measurement of Thermal Radiation Properties of Solids*, NASA SP-31, Session IV, pp. 425–431 (1963).

[4] Ward, L., "The variation with temperature of the spectral emissivities of iron, nickel and cobalt," Proc. Phys. Soc. (London) **69B**, 339–343 (1956).

[5] Price, D. J., "The emissivity of hot metals in the infrared," Proc. Phys. Soc. (London) **59**, 118–131 (1947).

[6] Reid, C., "Infrared reflectivities of nickel at high temperatures," Phys. Rev. **60**, 161 (1941).

[7] Hagen, E. and Rubens, H., "Uber Beziehungen des Reflexions und Emissionsvermögens der Metalle zu ihren Elektrischen Leitvermögen," Ann. Physik **11**, 873–901 (1903).

[8] Drude, P., *The Theory of Optics* (Longmans, Green and Co., New York, 1902), Chap. V, p. 382.

[9] Pappis, J. and Blum, S. L., "Properties of pyrolytic graphite," J. Am. Ceram. Soc. **44**, 592–597 (1961).

Visibility of a Lunar Satellite from an Earth Ground Station

P. R. Escobal*

TRW Space Technology Laboratories, Redondo Beach, Calif.

Introduction

ANALYSIS is presented for the solution of the visibility problem of a satellite of the moon from a ground station located on earth. The first portion of the line-of-sight communication problem is solved by obtaining a single transcendental equation in the eccentric anomaly of the lunicentered satellite.

Future space missions, specifically the conquest of the moon, as now envisioned under the Apollo project, present special communication problems. This paper investigates the optical or radar visibility of a satellite in an orbit about the moon from a specified station on the earth. The analysis is investigated from an astrodynamic point of view.

As will be seen, this problem becomes rather complex and should be separated into two different but related conditions that insure visibility of the lunar satellite. The first of these conditions, called herein the critical viewing time condition, i.e., when the satellite is not obscured by the bulge of the earth, is the problem attacked in this note. Condition two, the lunar eclipse situation, i.e., when the satellite is hidden by the moon, can be treated by a slight modification of eclipse theory.[4] Both conditions must be satisfied in order to insure a direct optical contact between the specified terrestrial station and the orbiting lunar satellite.

Critical Viewing Time Condition

Consider a ground station located in a geocentric, inertial coordinate system[1,2] illustrated in Fig. 1, with coordinates ϕ' and θ defined by $\phi' \equiv$ station geocentric latitude and $\theta \equiv$ station local sidereal time. The rectangular coordinates of the station coordinate radius vector $\mathbf{R}$ may be shown to be

$$X = -G_1 \cos\phi \cos\theta \qquad Y = -G_1 \cos\phi \sin\theta$$
$$Z = -G_2 \sin\phi \tag{1}$$

Received June 18, 1964; revision received January 11, 1965.

* Head, Special Studies Section. Member AIAA.

where, as developed in Ref. 1,

$$G_1 \equiv \frac{a_e}{[1 - (2f - f^2)\sin^2\phi]^{1/2}} + H$$

$$G_2 \equiv \frac{(1-f)^2 a_e}{[1 - (2f - f^2)\sin^2\phi]^{1/2}} + H$$

with the geodetic latitude ϕ defined by

$$\phi = \tan^{-1}[\tan\phi'/(1-f)^2] \qquad -(\pi/2) \leq \phi \leq (\pi/2)$$

and a_e = equatorial radius of earth, f = flattening of adopted ellipsoid, and H = station elevation above and measured normal to the surface of the adopted ellipsoid.

Consider the position of the moon defined in the same coordinate frame by vector $\mathbf{r}_m$, i.e., the position vector of the moon's center with respect to the geocenter. The coordinates of $\mathbf{r}_m$ can be obtained from the *American Ephemeris and Nautical Almanac*.[5] From the selenocenter, the position vector of a lunar satellite, $\mathbf{r}_s$, can be introduced and the vector $\mathbf{r}_c$ defined by

$$\mathbf{r}_c = \mathbf{R} + \mathbf{r}_m + \mathbf{r}_s \tag{2}$$

Figure 2 affords further clarification of the vector construction.

As can be seen from an observing station located at point A, it is always possible to observe satellite S, if S is itself not eclipsed by the moon. However, as the station rotates into position A' because of the sidereal rotation of the earth, a critical situation will be reached. This critical situation is of course caused by the line-of-sight interference of the earth, which has moved into a position between the lunar satellite and the observing station. For a spherical earth, the critical angle occurring at A' caused by line-of-sight interference is $\pi/2$, but for the sake of generality, and since the observing station may have definite observational constraints because of mountains, etc., let the critical angle be $\pi/2 + h$, where h is the minimum acceptable elevation angle of the observing station. For an oblate planet, h must be augmented by the angle ζ where

$$\zeta = \cos^{-1}\left[\frac{(G_1 \cos^2\phi + G_2 \sin^2\phi)}{R}\right] \qquad 0 \leq \zeta \leq \frac{\pi}{2}$$

In light of the previous discussion, the critical situation occurs when

$$\mathbf{r}_c \cdot \mathbf{R} = r_c R \cos(\pi/2 + h) = -r_c R \sin h \tag{3}$$

Substituting for $\mathbf{r}_c$ from Eq. (2) results in the relationship

$$(\mathbf{R} + \mathbf{r}_m + \mathbf{r}_s)\cdot\mathbf{R} = -r_c R \sin h \tag{4}$$

or

$$(\mathbf{r}_m + \mathbf{r}_s)\cdot\mathbf{R} = -R^2 - r_c R \sin h \tag{5}$$

Let the two unit vectors $\mathbf{P}_s$, $\mathbf{Q}_s$ be introduced where $\mathbf{P}_s$ is a vector pointing toward perigee of the lunicentered orbit, and $\mathbf{Q}_s$ is advanced to $\mathbf{P}_s$ by a right angle in the plane and direction of motion. Furthermore, if the lunicentered orbit

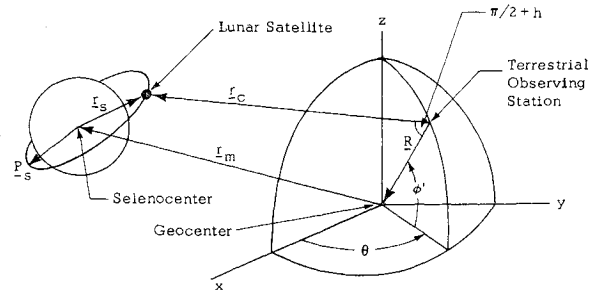

Fig. 1 Orbit geometry.